

## Superconductivity Emerging from an Electronic Phase Separation in the Charge Ordered Phase of $\text{RbFe}_2\text{As}_2$

E. Civardi,<sup>1</sup> M. Moroni,<sup>1</sup> M. Babij,<sup>2</sup> Z. Bukowski,<sup>2</sup> and P. Carretta<sup>1</sup>

<sup>1</sup>*Department of Physics, University of Pavia-CNISM, I-27100 Pavia, Italy*

<sup>2</sup>*Institute of Low Temperature and Structure Research, Polish Academy of Sciences, 50-422 Wroclaw, Poland*

(Received 11 August 2016; published 17 November 2016)

<sup>75</sup>As, <sup>87</sup>Rb, and <sup>85</sup>Rb nuclear quadrupole resonance (NQR) and <sup>87</sup>Rb nuclear magnetic resonance measurements in a  $\text{RbFe}_2\text{As}_2$  iron-based superconductor are presented. We observe a marked broadening of the <sup>75</sup>As NQR spectrum below  $T_0 \approx 140$  K which is associated with the onset of a charge order in the FeAs planes. Below  $T_0$  we observe a power-law decrease in the <sup>75</sup>As nuclear spin-lattice relaxation rate down to  $T^* \approx 20$  K. Below  $T^*$  the nuclei start to probe different dynamics owing to the different local electronic configurations induced by the charge order. A fraction of the nuclei probes spin dynamics associated with electrons approaching a localization while another fraction probes activated dynamics possibly associated with a pseudogap. These different trends are discussed in light of an orbital selective behavior expected for the electronic correlations.

DOI: 10.1103/PhysRevLett.117.217001

The parent compounds of high temperature superconducting cuprates are emblematic examples of Mott-Hubbard insulators at half band filling [1], where the large electron Coulomb repulsion  $U$  overcomes the hopping integral  $t$  and induces both charge localization and an antiferromagnetic (AF) coupling among the spins. Electronic correlations remain sizable even when the cuprates become superconducting and give rise to a rich phase diagram at low hole doping levels characterized by the onset of a charge density wave (CDW) which progressively fades away as the doping increases [2–5] and eventually, in the overdoped regime, a Fermi liquid scenario is restored. The comprehension of the role of electronic correlations in iron-based superconductors (IBSs) [6] is more subtle. At variance with the cuprates IBSs are characterized by similar nearest neighbor and next-nearest neighbor hopping integrals, the parent compounds of the most studied families of IBSs (e.g.,  $\text{BaFe}_2\text{As}_2$  and  $\text{LaFeAsO}$ ) [7] are not characterized by half-filled bands and, moreover, in IBSs the Fermi level typically crosses five bands associated with the different Fe  $3d$  orbitals, leading to a rich phenomenology in the normal as well as in the superconducting state [7,8]. Moreover, even if signs have been reported [9,10], the evidence for a charge order in the phase diagram of IBSs still remains elusive.

Nominally, half band filling can be approached in  $\text{BaFe}_2\text{As}_2$  IBSs by replacing Ba with an alkali atom  $A = \text{K}, \text{Rb}, \text{or Cs}$ , resulting in 5.5 electrons per Fe atom [11]. Transport measurements show that  $\text{AFe}_2\text{As}_2$  compounds are metals [12] with sizable electronic correlations and it has been recently pointed out that their behavior shares many similarities with that of heavy fermion compounds [12,13]. Indeed, the effective mass progressively increases as one moves from  $\text{BaFe}_2\text{As}_2$  to  $\text{AFe}_2\text{As}_2$  [14], even if clear discrepancies in the values derived by the

different techniques are found depending on their sensitivity to the electrons from a single band or from all the five bands [15]. de' Medici *et al.* [16] pointed out that if electronic correlations are sizable, namely,  $U/t$  is of the order of the unity, the local atomic physics starts to be relevant and Hund coupling may promote the single electron occupancy of Fe  $d$  orbitals (i.e., half band filling) and decouple the interband charge correlations. Accordingly, the Mott transition becomes orbital selective [16,17] so that while the electrons of a given band localize the electrons of other bands remain delocalized, leading to a metallic behavior and eventually to superconductivity. This orbital selective behavior should give rise to markedly  $k$ -dependent response functions [18] and to a sort of  $k$ -space phase separation of metallic and insulating-like domains. The point is, what happens in the real space? Will one probe the sum of the insulating and metallic response functions or should one detect a real space phase separation [19] also in the  $\text{AFe}_2\text{As}_2$  IBS [20], with different local susceptibilities? More interestingly, if electronic correlations become significant in  $\text{AFe}_2\text{As}_2$  one could envisage the onset of a charge order [21] as in the cuprates [2–5].

Nuclear quadrupole resonance (NQR) and nuclear magnetic resonance (NMR) are quite powerful tools which allow us to probe the local response function and charge distribution. Moreover, in NQR experiments [22] the magnetic field, which often acts as a relevant perturbation, is zero. Here we show, by combining <sup>75</sup>As and <sup>87,85</sup>Rb NQR and <sup>87</sup>Rb NMR measurements, that in  $\text{RbFe}_2\text{As}_2$  a charge order develops in the normal state below  $T_0 \approx 140$  K, possibly leading to a differentiation in real space of Fe atoms with different orbital configurations. Below  $T_0$ , <sup>75</sup>As and <sup>87</sup>Rb nuclear spin-lattice relaxation rates ( $1/T_1$ ) show a power law behavior, as it is expected for a strongly

correlated electron system and in good agreement with  $^{75}\text{As}$  NMR results reported by Wu *et al.* [13]. However, at  $T^* \approx 20$  K we observe that a fraction of  $^{75}\text{As}$  (or  $^{87}\text{Rb}$ ) nuclei probes spin dynamics characteristic of a system approaching localization while others probe dynamics possibly associated with a metallic phase with a pseudogap [23–25]. Upon further decreasing the temperature the volume fraction of the heavy electron phase vanishes while the one of the metallic phase, which eventually becomes superconducting below  $T_c \approx 2.7$  K, grows. Thus, we present neat evidence for a charge order in  $\text{RbFe}_2\text{As}_2$  akin to underdoped cuprates. The charge order favors a phase separation into metallic and nearly insulating regions, which could result from the theoretically predicted orbital selective behavior [16].

NQR and NMR measurements were performed on a  $\text{RbFe}_2\text{As}_2$  polycrystalline sample with a mass of about 400 mg, sealed in a quartz tube under a 0.2 bar Ar atmosphere in order to prevent deterioration. The superconducting transition temperature derived from ac susceptibility measurements turned out  $T_c \approx 2.7$  K, in good agreement with previous findings [26,27]. Further details on the sample preparation and characterization are given in the Supplemental Material [28].

First of all we shall discuss the appearance of a charge order in the FeAs planes of  $\text{RbFe}_2\text{As}_2$ , as detected by  $^{75}\text{As}$  NQR spectra. For a nuclear spin  $I = 3/2$ , as it is the case of  $^{75}\text{As}$  and  $^{87}\text{Rb}$ , the NQR spectrum is characterized by a single line at a frequency [22]

$$\nu_Q = \frac{eQV_{ZZ}}{2h} \left( 1 + \frac{\eta^2}{3} \right)^{1/2}, \quad (1)$$

with  $Q$  the nuclear quadrupole moment,  $V_{ZZ}$  the main component of the electric field gradient (EFG) tensor, and  $\eta$  its asymmetry  $\eta = (V_{XX} - V_{YY})/V_{ZZ}$ . Hence, the NQR spectrum probes the EFG at the nuclei generated by the surrounding charge distribution. Above 140 K, the  $^{75}\text{As}$  NQR spectrum (Fig. 1) is centered around 14.6 MHz, with a linewidth of about 170 kHz, while the  $^{87}\text{Rb}$  NQR spectrum is centered around 6.2 MHz with a width of about 20 kHz. The relatively narrow NQR spectra confirms the good quality of our sample. We performed density functional theory (DFT) calculations using the ELK code in the generalized gradient approximation [28] in order to derive *ab initio* the electric field gradient and NQR frequency. For  $^{75}\text{As}$  and  $^{87}\text{Rb}$  we obtained  $(^{75}\nu_Q)_{\text{DFT}} = 14.12$  MHz and  $(^{87}\nu_Q)_{\text{DFT}} = 6.7$  MHz, respectively, in reasonable agreement with the experimental values in spite of the significant electronic correlations [37]. This shows that DFT is still able to provide a fair description of the system as far as it remains a normal metal.

Upon cooling the sample below  $T_0 \approx 140$  K significant changes are detected in the  $^{75}\text{As}$  NQR spectra (Fig. 1). The spectrum is observed to progressively broaden with

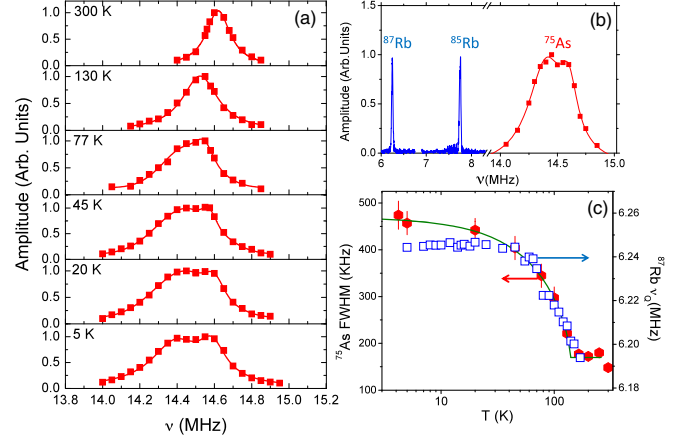


FIG. 1. (a) The  $^{75}\text{As}$  NQR spectrum in  $\text{RbFe}_2\text{As}_2$  is reported at different temperatures between 5 K and 300 K. The red lines are best fits with one or two (for  $T < 130$  K) Lorentzians. (b) The merge of the NQR spectra, associated with the  $m_I = \pm 3/2 \rightarrow \pm 1/2$  transition for  $^{75}\text{As}$  and  $^{87}\text{Rb}$  and with the  $m_I = \pm 5/2 \rightarrow \pm 3/2$  transition for  $^{85}\text{Rb}$  ( $I = 5/2$ ), is shown for  $T = 4.2$  K. The intensity of the three spectra has been rescaled so that all three spectra have similar intensities. (c) The temperature dependence of the full width at half intensity (FWHM) of  $^{75}\text{As}$  NQR spectra (red octagons, left scale, for the plot with linear  $T$  scale see the Supplemental Material [28]) is shown together with the temperature dependence of  $^{87}\text{Rb}$   $\nu_Q$  (blue squares, right scale). The green solid line tracking the order parameter is a phenomenological fit of the FWHM ( $\Delta\nu_Q$ ) with  $\Delta\nu_Q = 300[1 - (T/T_0)]^\beta + 170$  kHz, with  $T_0 = 140$  K and  $\beta \approx 0.7$ .

decreasing temperature and below 50 K one clearly observes that the spectrum is actually formed by two humps nearly symmetrically shifted with respect to the center [Fig. 1(a)]. The presence of two peaks in the  $^{75}\text{As}$  NQR spectra has already been detected in different families of IBSSs and associated with a nanoscopic phase separation in regions characterized by different electron doping levels [38]. However, at variance with what we observe here, the two peaks observed in other IBSSs do not show the same intensity [38] and the spectra show little temperature dependence, namely, the nanoscopic phase separation is likely pinned. Under both high magnetic field and high pressure an asymmetric splitting of the  $^{75}\text{As}$  NMR spectrum was detected also in  $\text{KFe}_2\text{As}_2$  which, however, is absent in zero field (NQR) [10]. Here we observe the emergence of a NQR spectrum which recalls the one expected for an incommensurate CDW [39–41], which causes a periodic modulation of the EFG at the nuclei and gives rise to two symmetrically shifted peaks in the spectrum. The EFG modulation could involve also the onset of an orbital order [42] or a structural distortion, possibly coupled to the charge order. Although it is not straightforward from our data to discriminate among these scenarios, it is clear that we detect a symmetry breaking below  $T_0$  to a low temperature phase characterized by

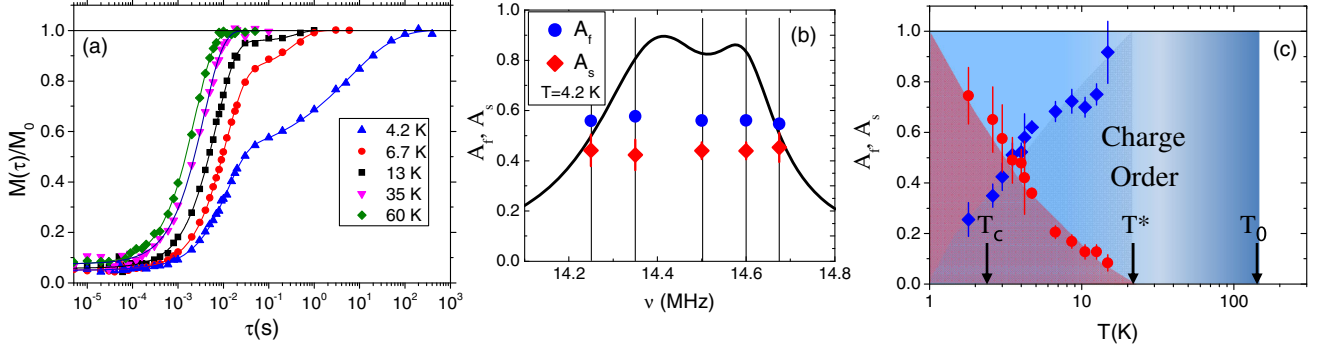


FIG. 2. (a) The recovery of  $^{75}\text{As}$  nuclear magnetization  $M(\tau)$  (measured in NQR) is reported as a function of the delay  $\tau$  between a saturation radio frequency pulse sequence and the echo readout sequence for different temperatures. The solid lines are the best fits according to Eq. (2) in the text. (b) The frequency dependence of the fraction of fast  $A_f$  and slow relaxing  $A_s$  nuclei is reported as a function of the irradiation frequency across the  $^{75}\text{As}$  NQR spectrum. The black solid line is the best fit of the spectrum at  $T = 4.2$  K. (c) The temperature dependence of  $A_f$  (blue) and  $A_s$  (red) recorded on the low-frequency peak of the  $^{75}\text{As}$  NQR spectrum.

a spatial modulation of the EFG, namely, by a charge order.

The  $^{87}\text{Rb}$  NQR spectrum does not show a significant broadening upon decreasing the temperature but is characterized by a  $\nu_Q$  which, at  $T > T^* \approx 20\text{--}25$  K, shows a temperature dependence similar to that of the  $^{75}\text{As}$  NQR spectra full width at half maximum (FWHM), proportional to the charge order parameter [Fig. 1(c)]. Below  $T^*$   $^{87}\text{Rb}$   $\nu_Q$  flattens and deviates from  $^{75}\text{As}$  NQR FWHM. The fact that the NQR spectrum of the out of plane  $^{87}\text{Rb}$  nuclei is less sensitive than the  $^{75}\text{As}$  one to the charge order is an indication that the order develops in the FeAs planes and that the modulation of the EFG at  $^{75}\text{As}$  nuclei should occur over a few lattice steps, otherwise one should expect a splitting also of the narrow  $^{87}\text{Rb}$  NQR spectrum. It is interesting to notice that at a temperature of the order of  $T^*$  an abrupt change in the uniaxial thermal expansion occurs [43], evidencing also a change in the lattice properties.

Now we discuss the temperature dependence of the low-energy dynamics probed by  $^{75}\text{As}$  and  $^{87}\text{Rb}$   $1/T_1$ . The nuclear spin-lattice relaxation rate was determined from the recovery of the nuclear magnetization after exciting the nuclear spins with a saturation recovery pulse sequence. The recovery of  $^{75}\text{As}$  magnetization in NQR is shown in Fig. 2(a). One notices that a single exponential recovery describes very well the recovery of the nuclear magnetization at  $T \geq 20$  K, as it can be expected for a homogeneous system where all nuclei probe the same dynamics. However, below  $T^* \approx 20$  K one observes the appearance of a second component characterized by much longer relaxation times. Namely, a part of the nuclei probes dynamics causing a fast relaxation ( $1/T_1^f$ ) and a part of the nuclei a slow relaxation ( $1/T_1^s$ ). Accordingly, the recovery was fit to

$$M(\tau) = M_0 \left[ 1 - f \left( A_f e^{-3\tau/T_1^f} + A_s e^{-(3\tau/T_1^s)^\beta} \right) \right], \quad (2)$$

with  $M_0$  the nuclear magnetization at thermal equilibrium,  $A_f$  and  $A_s$  the fraction of fast relaxing and slow relaxing nuclei, respectively,  $f$  a factor accounting for a nonperfect saturation by the radio frequency pulses, and  $0.8 \geq \beta \geq 0.3$  a stretching exponent characterizing the slowly relaxing component. As the temperature is lowered one observes a progressive increase of  $A_s$  with respect to  $A_f$  and at the lowest temperature ( $T = 1.7$  K), about 80% of the nuclei are characterized by the slow relaxation [Fig. 2(c)]. It is important to notice that in  $\text{RbFe}_2\text{As}_2$ , Wu *et al.* [13] (in NMR, not in NQR) did not observe a clear separation of the recovery in two components as we do here but they did observe deviations from a single exponential recovery below 20 K which, however, were fitted with a stretched exponential, likely yielding an average  $1/T_1$  value between  $1/T_1^s$  and  $1/T_1^f$ . Remarkably,  $^{87}\text{Rb}$  NMR  $1/T_1$  also clearly shows two components below 25 K and just one above [28].

$^{75}\text{As}$   $1/T_1$  was measured both on the high-frequency and on the low-frequency shoulder of the NQR spectrum and it was found to be the same [Fig. 3(a)] over a broad temperature range. Moreover, at  $T = 4.2$  K we carefully checked the frequency dependence of  $T_1^f$ ,  $T_1^s$ ,  $A_f$ , and  $A_s$  and found that neither the two relaxation rates nor their amplitude vary across the spectrum (Fig. 2(b), see also Ref. [28]). This means that nuclei resonating at different frequencies probe the same dynamics which implies that the charge modulation induced by the charge order has a nanoscopic periodicity [38]. One could argue that the two components are actually present at all temperatures but that they arise only at a low temperature once nuclear spin diffusion [44] is no longer able to establish a common spin temperature (i.e., a common  $T_1$ ) among the nuclei resonating at different frequencies. However, we remark that since the nuclear spin-spin relaxation rate ( $1/T_2$ ) is constant [28] and the width of the NQR spectrum is nearly constant below 40 K [Fig. 1(c)] the poor efficiency of nuclear spin diffusion should not vary, at least for  $T \leq 40$  K. Hence, the

appearance of different relaxation rates below  $T^*$  should arise from a phase separation causing a slight change in the average electronic charge distribution and little effect on the NQR spectra (see Fig. 1) but a marked differentiation in the low-energy excitations [18], which starts to be significant at low temperature once the electronic correlations are relevant.

One has to clarify if the relaxation mechanism is magnetic, driven by electron spin fluctuations, or quadrupolar, driven by EFG fluctuations, typically induced by CDW amplitude and phase modes [41]. In order to clarify this point, we measured the ratio between  $^{87}\text{Rb}$  and  $^{85}\text{Rb}$   $1/T_1$  (fast component) at a few selected temperatures below 25 K. The ratio  $^{87}(1/T_1)/^{85}(1/T_1) = 12 \pm 1$ , in good agreement with the ratio between the square of the gyromagnetic ratios of the two nuclei  $(^{87}\gamma/^{85}\gamma)^2 = 11.485$ , showing that the relaxation is driven by the correlated spin fluctuations and not by charge fluctuations associated with CDW excitations. Since  $^{75}\text{As}$  shows a temperature dependence of the relaxation analogous to the one of  $^{87}\text{Rb}$  [Fig. 3(a)] we argue that  $^{75}\text{As}$   $1/T_1$  is also driven by spin fluctuations. Thus we can write that

$$\frac{1}{T_1} = \frac{\gamma_n^2}{2\hbar} k_B T \frac{1}{N} \sum_{\vec{q}} |A_{\vec{q}}|^2 \frac{\chi''(\vec{q}, \omega_0)}{\omega_0}, \quad (3)$$

with  $|A_{\vec{q}}|^2$  the form factor giving the hyperfine coupling with the collective spin excitations at wave vector  $\vec{q}$ , and  $\chi''(\vec{q}, \omega_0)$  the imaginary part of the dynamic susceptibility at the resonance frequency  $\omega_0$ .

Now we turn to the temperature dependence of  $1/T_1$  above  $T^* \simeq 20$  K and of  $1/T_1^s$  and  $1/T_1^f$  below that temperature. Above  $T^*$ ,  $1/T_1$  increases with a power law  $1/T_1 = aT^b$ , with  $b = 0.79 \pm 0.01$  for  $^{75}\text{As}$ , and flattens around  $T_0 \simeq 140$  K [Fig. 3(a)], in very good agreement with the results reported by Wu *et al.* [13] from  $^{75}\text{As}$  NMR. Notice that  $T_0$  corresponds to the temperature below which we start to observe a significant broadening of the  $^{75}\text{As}$  NQR spectrum. Hence, the power law behavior of  $1/T_1$  seems to arise from the onset of the charge order.

Below  $T^* \simeq 20$  K,  $1/T_1^f$  deviates from the power law behavior and progressively flattens on decreasing temperature [Fig. 3(a)]. The same behavior is detected for  $^{87}\text{Rb}$  NMR  $1/T_1$ , although the flattening starts at a higher temperature, suggesting that  $T^*$  might be field dependent. On the other hand,  $1/T_1^s$  gets progressively longer as the temperature is lowered and follows an activated trend with an energy barrier  $E_g = 17 \pm 0.9$  K.

The behavior of  $1/T_1^f$  is characteristic of a system approaching a quantum critical point (QCP) where localization occurs. In fact, from the Moriya self-consistent renormalization (SCR) approach for a quasi-2D system with AF correlations, one should have  $1/T_1 = T\chi(Q)$  [45,46], with  $\chi(Q)$  the static susceptibility at the AF wave vector. In the proximity of the QCP  $\chi(Q) \sim \ln(1/T)/T$ ,

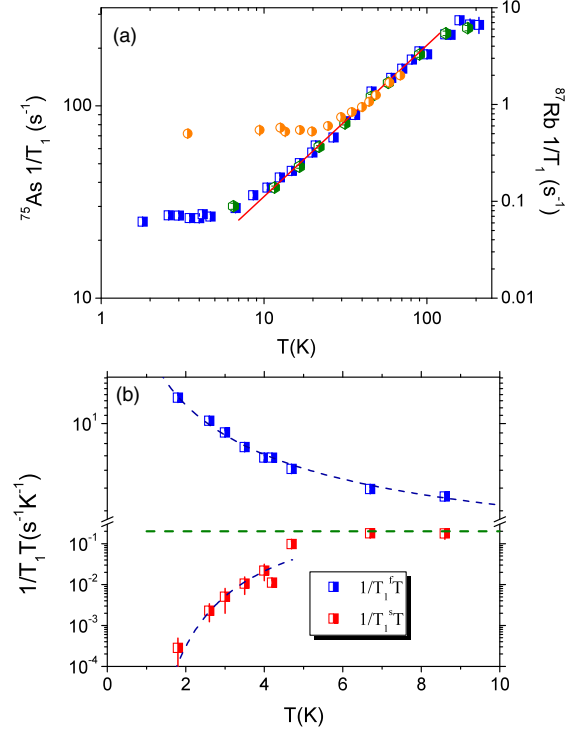


FIG. 3. (a) The temperature dependence of  $^{75}\text{As}$  NQR  $1/T_1$  in  $\text{RbFe}_2\text{As}_2$ , for  $T \geq 20$  K, and of the fast relaxation rate  $1/T_1^f$ , for  $T < 20$  K, are reported for an irradiation frequency centered at the low-frequency peak (blue squares) and for an irradiation frequency centered at the high frequency peak (green circles). The red solid line is a best fit to the data between 20 and 100 K with a power law characterized by an exponent  $b = 0.79$ .  $^{87}\text{Rb}$  NMR  $1/T_1$  (orange circles) in  $\text{RbFe}_2\text{As}_2$  is reported between 3.5 and 70 K, for an external magnetic field  $H = 7$  Tesla. (b) The temperature dependence of  $^{75}\text{As}$  NQR  $1/T_1^f T$  (blue squares) and  $1/T_1^s T$  (red circles) in  $\text{RbFe}_2\text{As}_2$  is reported. The dashed line at the bottom is the best fit according to an activated behavior with an energy gap  $E_g = 17 \pm 0.9$  K. The dashed line at the top is the behavior expected according to Moriya SCR theory (see text). The dashed horizontal line shows schematically the Korringa-like behavior expected for an uncorrelated metal.

leading to a weak logarithmic divergence of  $1/T_1 \sim \ln(1/T)$  for  $T \rightarrow 0$ , while at higher temperature  $\chi(Q)$  should show a Curie-Weiss behavior, yielding a nearly flat  $1/T_1$ , as we do observe in  $\text{RbFe}_2\text{As}_2$  [Fig. 3(a)]. The corresponding behavior of  $1/T_1^f T$  is reported in Fig. 3(b).

On the other hand,  $1/T_1^s T$ , corresponding to the relaxation rate of the majority phase at low temperature, shows the opposite trend [Fig. 3(b)], decreasing upon cooling. Being the system metallic at low temperature, the deviation of  $1/T_1^s T$  from the constant Korringa-like behavior [22] expected for a metal should possibly be associated with the opening of a pseudogap, similarly to what one observes in the underdoped regime of the cuprates [23–25], and in agreement with theoretical predictions for hole-doped IBSSs [18].

In conclusion, our results show that, akin to cuprates, a charge order develops also in the normal state of IBSSs when the electronic correlations are sizable. Accordingly, the presence of a charge order appears to be a common feature in the phase diagram of cuprate and iron-based superconductors and could play a key role in determining the superconducting state properties [21,47]. Moreover, we observe a local electronic separation in two phases characterized by different excitations which could possibly be explained in terms of the orbital selective behavior [16] predicted for IBSSs. Finally, we remark that the occurrence of an electronic phase separation is theoretically supported by a recent study of the electron fluid compressibility [48].

Massimo Capone is thanked for useful discussions. The Sezione INFN di Pavia is acknowledged for granting the computing time necessary to perform DFT calculations. This work was supported by MIUR (Ministero dell'Istruzione, dell'Università e della Ricerca Scientifica) Project PRIN2012 No. 2012X3YFZ2.

- 
- [1] N. F. Mott, *Proc. Phys. Soc. London Sect. A* **62**, 416 (1949).  
 [2] T. Wu, H. Mayaffre, S. Krämer, M. Horvatić, C. Berthier, W. N. Hardy, R. Liang, D. A. Bonn, and M.-H. Julien, *Nature (London)* **477**, 191 (2011).  
 [3] J. M. Tranquada, B. J. Sternlieb, J. D. Axe, Y. Nakamura, and S. Uchida, *Nature (London)* **375**, 561 (1995).  
 [4] G. Ghiringhelli *et al.*, *Science* **337**, 821 (2012).  
 [5] M. Hücker *et al.*, *Phys. Rev. B* **90**, 054514 (2014).  
 [6] Y. Kamihara, T. Watanabe, M. Hirano, and H. Hosono, *J. Am. Chem. Soc.* **130**, 3296 (2008).  
 [7] D. C. Johnston, *Adv. Phys.* **59**, 803 (2010).  
 [8] I. I. Mazin, D. J. Singh, M. D. Johannes, and M. H. Du, *Phys. Rev. Lett.* **101**, 057003 (2008); K. Kuroki, S. Onari, R. Arita, H. Usui, Y. Tanaka, H. Kontani, and H. Aoki, *Phys. Rev. Lett.* **101**, 087004 (2008).  
 [9] A. K. Jasek, K. Komadera, A. Blachowski, K. Ruebenbauer, Z. Bukowski, J. G. Storey, and J. Karpinski, *J. Alloys Compd.* **609**, 150 (2014).  
 [10] P. S. Wang, P. Zhou, J. Dai, J. Zhang, X. X. Ding, H. Lin, H. H. Wen, B. Normand, R. Yu, and W. Yu, *Phys. Rev. B* **93**, 085129 (2016).  
 [11] F. F. Tafti, A. Ouellet, A. Juneau-Fecteau, S. Faucher, M. Lapointe-Major, N. Doiron-Leyraud, A. F. Wang, X.-G. Luo, X. H. Chen, and L. Taillefer, *Phys. Rev. B* **91**, 054511 (2015).  
 [12] F. Eilers *et al.*, *Phys. Rev. Lett.* **116**, 237003 (2016).  
 [13] Y. P. Wu, D. Zhao, A. F. Wang, N. Z. Wang, Z. J. Xiang, X. G. Luo, T. Wu, and X. H. Chen, *Phys. Rev. Lett.* **116**, 147001 (2016); see also the corresponding Supplemental Material at <http://link.aps.org/supplemental/10.1103/PhysRevLett.117.217001>.  
 [14] A. K. Pramanik, M. Abdel-Hafiez, S. Aswartham, A. U. B. Wolter, S. Wurmehl, V. Kataev, and B. Büchner, *Phys. Rev. B* **84**, 064525 (2011).  
 [15] G. Li, W. Z. Hu, J. Dong, Z. Li, P. Zheng, G. F. Chen, J. L. Luo, and N. L. Wang, *Phys. Rev. Lett.* **101**, 107004 (2008); M. Yi *et al.*, *Phys. Rev. B* **80**, 024515 (2009).  
 [16] L. de' Medici, S. R. Hassan, M. Capone, and X. Dai, *Phys. Rev. Lett.* **102**, 126401 (2009).  
 [17] L. de' Medici, G. Giovannetti, and M. Capone, *Phys. Rev. Lett.* **112**, 177001 (2014).  
 [18] E. Gull, M. Ferrero, O. Parcollet, A. Georges, and A. J. Millis, *Phys. Rev. B* **82**, 155101 (2010).  
 [19] V. J. Emery and S. A. Kivelson, *Physica C (Amsterdam)* **209C**, 597 (1993); U. Low, V. J. Emery, K. Fabricius, and S. A. Kivelson, *Phys. Rev. Lett.* **72**, 1918 (1994).  
 [20] E. Dagotto, A. Moreo, A. Nicholson, Q. Luo, S. Liang, and X. Zhang, *Front. Phys.* **6**, 379 (2011).  
 [21] C. Castellani, C. Di Castro, and M. Grilli, *Phys. Rev. Lett.* **75**, 4650 (1995).  
 [22] A. Abragam, in *Principles of Nuclear Magnetism* (Oxford University Press, New York, 1983).  
 [23] H. Alloul, T. Ohno, and P. Mendels, *Phys. Rev. Lett.* **63**, 1700 (1989).  
 [24] H. Ding, T. Yokoya, J. C. Campuzano, T. Takahashi, M. Randeria, M. R. Norman, T. Mochiku, H. Kadowaki, and J. Giapintzakis, *Nature (London)* **382**, 51 (1996).  
 [25] B. Batlogg, H. Y. Hwang, H. Takagi, R. J. Cava, H. L. Kao, and J. Kwo, *Physica (Amsterdam)* **235-240C**, 130 (1994).  
 [26] Z. Bukowski, S. Weyeneth, R. Puzniak, J. Karpinski, and B. Batlogg, *Physica (Amsterdam)* **470C**, S328 (2010).  
 [27] Z. Shermadini, H. Luetkens, A. Maisuradze, R. Khasanov, Z. Bukowski, H.-H. Klauss, and A. Amato, *Phys. Rev. B* **86**, 174516 (2012).  
 [28] See the Supplemental Material at <http://link.aps.org/supplemental/10.1103/PhysRevLett.117.217001> for details on the sample preparation and characterization, DFT calculations as well as on NQR and NMR measurements, which includes Refs. [29–36].  
 [29] ELK code, version 3.3.17, <http://elk.sourceforge.net>.  
 [30] J. P. Perdew, A. Ruzsinszky, G. I. Csonka, O. A. Vydrov, G. E. Scuseria, L. A. Constantin, X. Zhou, and K. Burke, *Phys. Rev. Lett.* **100**, 136406 (2008).  
 [31] H. J. Monkhorst and J. D. Pack, *Phys. Rev. B* **13**, 5188 (1976).  
 [32] M. Methfessel and A. T. Paxton, *Phys. Rev. B* **40**, 3616 (1989).  
 [33] J. A. Lehmann-Horn, R. Yong, D. G. Miljak, and T. J. Bastow, *Solid State Nucl. Magn. Reson.* **71**, 87 (2015).  
 [34] R. E. Walstedt and S.-W. Cheong, *Phys. Rev. B* **51**, 3163 (1995).  
 [35] L. Bossoni, P. Carretta, W. P. Halperin, S. Oh, A. Reyes, P. Kuhns, and P. C. Canfield, *Phys. Rev. B* **88**, 100503 (2013).  
 [36] D. E. MacLaughlin, J. D. Williamson, and J. Butterworth, *Phys. Rev. B* **4**, 60 (1971).  
 [37] S. Backes, H. O. Jeschke, and R. Valenti, *Phys. Rev. B* **92**, 195128 (2015).  
 [38] G. Lang, H.-J. Grafe, D. Paar, F. Hammerath, K. Manthey, G. Behr, J. Werner, and B. Büchner, *Phys. Rev. Lett.* **104**, 097001 (2010).  
 [39] P. Butaud, P. Ségransan, C. Berthier, J. Dumas, and C. Schlenker, *Phys. Rev. Lett.* **55**, 253 (1985).  
 [40] J. H. Ross, Z. Wang, and C. P. Slichter, *Phys. Rev. Lett.* **56**, 663 (1986).

- [41] C. Berthier and P. Ségransan, in *Low-dimensional Conductors and Superconductors*, edited by D. Jérôme and L. G. Caron (Plenum, New York, 1987), p. 455.
- [42] K. I. Kugel and D. I. Khomskii, *Sov. Phys. JETP* **37**, 725 (1973).
- [43] F. Hardy *et al.*, [arXiv:1605.05485](https://arxiv.org/abs/1605.05485) [*Phys. Rev. B* (to be published)].
- [44] W. E. Blumberg, *Phys. Rev.* **119**, 79 (1960).
- [45] A. Ishigaki and T. T. Moriya, *J. Phys. Soc. Jpn.* **65**, 3402 (1996); **67**, 3924 (1998).
- [46] F. Hammerath, P. Bonfá, S. Sanna, G. Prando, R. De Renzi, Y. Kobayashi, M. Sato, and P. Carretta, *Phys. Rev. B* **89**, 134503 (2014).
- [47] S. Caprara, C. Di Castro, G. Seibold, and M. Grilli, [arXiv:1604.07852v1](https://arxiv.org/abs/1604.07852v1).
- [48] L. de' Medici, [arXiv:1609.01303v1](https://arxiv.org/abs/1609.01303v1).